Power Transfer by Non Radiative Electromagnetic Fields between High-Q Resonant Coupled Circuits

José Alberty

Department of Science and Technology Industries, University of Applied Sciences of Western Switzerland, Rue de la Prairie 4, CH-1202 Genève, Switzerland; *jose.alberty@hesge.ch*

Simulation Notes Europe SNE 23(1), 2013, 31 - 38
DOI: 10.11128/sne.23.tn.10169
Received: Feb. 10, 2012 (Selected ASIM STS 2011 Postconf. Publ.); Revised Accepted: March 20, 2013;

Abstract. Between two high quality-factor (Q) resonant magnetically coupled circuits, non-radiative power transfer is modelled and observed in agreement with predictions found in recent works from MIT. The physical behaviour of the receptor as well as the geometry of the power flux lines (Poynting) are explained in terms of general behaviour of the power flux near completely absorbing targets. Practical consequences are extracted and generalisations of the source-receptors' geometries are proposed.

Introduction

It was recently shown [7], [6] that strongly coupled oscillating electrical circuits at resonance having high Q factors, are able of exchanging electromagnetic power in ways which are markedly different from more common coupled circuits, such as primary and secondary circuits in a transformer or even close emitter-receptor antennae pairs. What distinguishes power exchanges in traditional devices from those in the new ones relates to the way in which the power flux organizes itself geometrically between the source/emitter and the target/receiver regions. This particular organisation is a result of the interplay between the wave character of the field and the conditions of near-perfect wave absorption which are met at the receptor level at resonance. In this sense the same type of qualitative phenomena are found in all domains where strong wave absorption occurs (optical waves around totally absorbing bodies, particle wave function in the neighbourhood of resonant nuclei, etc.).

A complete analytical model is developed under the assumption of large electromagnetic wavelengths λ, compared to the set-up characteristic dimensions.

On the modelling and simulation side, we extensively used *Mathematica* to develop the entire analytical model and to visualise the fields and the fluxes in 3D, to compute - symbolically and numerically - the iterative solutions to the mixed induction-law equations and to interactively explore the space of parameters available in the this type of physics problem. This latter facility offered by this software was very helpful in understanding the physical subtleties involved in this type of systems. Finally the possibility offered by *Mathematica* of defining functions with generic arguments which remain unevaluated until called for by numerical or functional operations, allowed for changes in the definition of these arguments at later stages in the modelling chain, changes which are immediately and automatically impacted on all intermediate stages of the chain, without the need to redefine the original function for each new type of argument (reusable functions).

1 Setup Parameters and Geometry

In this work we consider a system made of one or more copper solenoids, represented by loops of radius $b = 5.5\ [cm]$ and diameter $a = 1.5\ [mm]$, even if each solenoid may contain more than one loop. Actually we use 5.5 turns per coil. At least one of the solenoids - the reference solenoid - is always present, located on the OXY -plane and centred at the origin O of the axis (see Figure 1).

We will use polar and Cartesian coordinates, depending on the type of calculation needed. For a general point P in space, these coordinates are shown in Figure 1. To begin with and for the sake of comparison with later results, we model the electro- magnetic field generated by an alternating current in the reference loop at frequencies $f1 = 5\ [MHz]$ and $f2 = 35\ [MHz]$, neglecting its inductive, capacitive and ohmic characteristics.

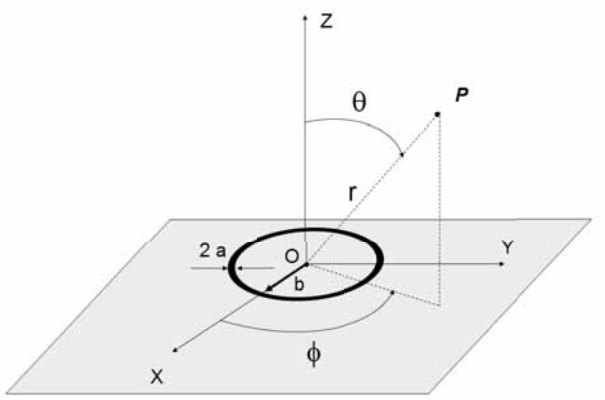

Figure 1: Cartesian (X,Y,Z) and polar (r,ϕ,θ) coordinates of a point P. The horizontal circle of radius b is a single conduction loop of diameter $2\cdot a$.

Later we will model the interaction of an external field with the reference solenoid. The full impedance elements of the solenoid's equivalent circuit must then be taken into account. For a solenoid with the characteristics indicated above, the inductance will be $L = 7.7\ [\mu H]$. We model the capacity C as a tunable capacity fixed at $C = 3.3\ [nF]$ in series with L and with the total resistance which is quite small ($R = 0.01\ [\Omega]$) and mainly due to the wire' s ohmic surface resistance per turn(We will neglect the presence of distributed capacities and radiative resistance.). The RLC oscillating circuit formed by the solenoid, the capacity and the resistance will thus resonate at frequency $f_{res} = \frac{1}{2\pi\sqrt{LC}} = 998'649\ [Hz]$.

2 Fields and Power Fluxes

The physics behind the phenomena which interest us here are simply Biot-Savart's and Faraday-Lenz's induction laws, iterated several times. An important assumption we make is that the magnetic fields' wavelength must be far larger than the typical circuits dimensions. This amounts to saying that the current distributions inside each circuit may safely be considered as being uniform along the circuits' length. If this condition is not met, our results will not be generally correct. The present modelling approach is similar to [3]. However our main interest relates to the dynamics of the electromagnetic field in the entire space and its relation to the effect of power flux concentration at resonances.

2.1 Single solenoid source

At an arbitrary point P in free space, with coordinates (r,ϕ,θ), the electromagnetic field created by an oscillating uniform current of frequency f and peak intensity I, circulating inside an horizontal (XY plane) conducting loop of radius b, made of wire of radius a and centered at the origin, is given by [1]

$$\begin{aligned} H_r &= H_r(f,I,\theta,r) \\ &= \frac{\imath\, k b^2 I cos\theta}{2r^2}\, e^{-\imath k r}\left(1-\frac{\imath}{k r}\right) \qquad (1) \\ H_\theta &= H_\theta(f,I,\theta,r) \\ &= -\frac{(k b)^2 I sin\theta}{4r}\, e^{-\imath k r}\left(1-\frac{\imath}{k r}-\frac{1}{(k r)^2}\right) \qquad (2) \\ E_\phi &= E_\phi(f,I,\theta,r) \\ &= \eta\,\frac{(k b)^2 I sin\theta}{4r}\, e^{-\imath k r}\left(1-\frac{\imath}{k r}\right) \qquad (3) \end{aligned}$$

where H_r and H_θ denote the radial and zenith components of the magnetic field and E_ϕ is the azimuthal component of the electric field at P. Here $k = \frac{2\pi}{\lambda}$ is the field's wave-number and $\eta = \sqrt{\frac{\mu_0}{\eta_0}}$ the vacuum impedance.

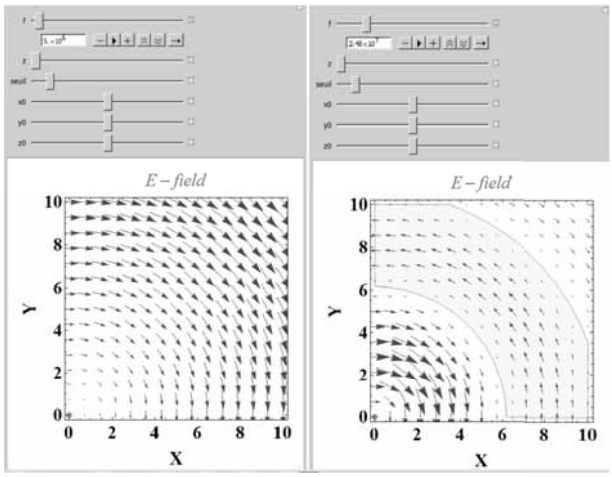

Figure 2: E-field lines at frequencies f_1 and f_2 in the XY-plane. Coloured sector (yellow) corresponds to $E_\phi > 0$. The solenoid is indicated by a fat red dot at the origin representing its center.

The E and H-field lines are shown in Figure 2 and Figure 3.

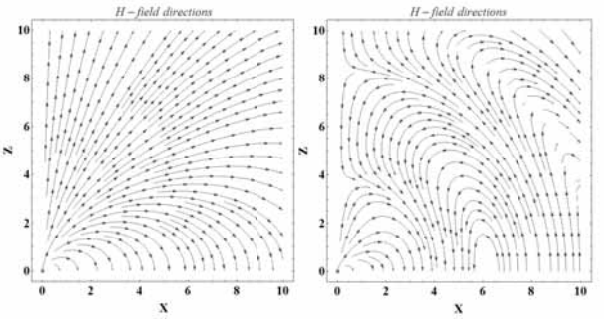

Figure 3: H-field lines at frequencies f_1 and f_2 in the XZ-plane.

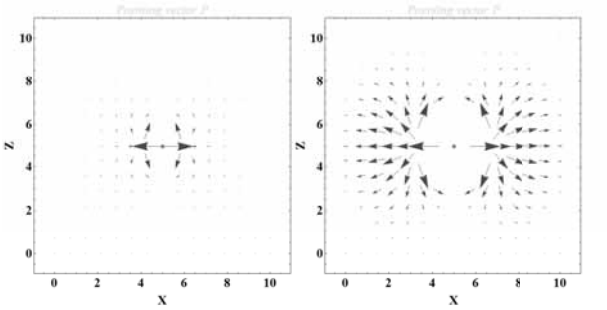

Figure 4: Poynting vector field (power flux) in the XZ-plane under the same conditions as in Figures 2 and 3. Arrow lengths are proportional to the power flux intensities (Poynting norm).

The power fluxes are determined by using the *Poynting vector*, defined as

$$\vec{P} = \Re\vec{E} \wedge \Re\vec{H} \tag{4}$$

where the Cartesian expressions of the E and H-fields in the XY and XZ-planes are obtained from the field components in equation (1) after rotating by the angles ϕ and θ respectively:

$$\vec{E} = R_z(\phi)\ \{0, E_\phi, 0\} \tag{5}$$
$$\vec{H} = R_y(\theta)\ \{H_r, 0, H_\theta\} \tag{6}$$

where $R_z(\phi) = \begin{pmatrix} cos\phi & -sin\phi & 0 \\ sin\phi & cos\phi & 0 \\ 0 & 0 & 1 \end{pmatrix}$ and $R_y(\theta) = \begin{pmatrix} sin\theta & 0 & cos\theta \\ 0 & 1 & 0 \\ cos\theta & 0 & -sin\theta \end{pmatrix}$.

For future reference, the power flux lines (field of Poynting vectors) at frequencies f_1 and f_2 are shown in Figure 4. The maximal power fluxes occur on the loop plane and the minimal (zero) flux is perpendicular to this plane near the loop, in agreement with the typical shape of power distribution polar diagrams for small loop antennas.

3 Single Coil in an External Magnetic Field

3.1 Uniform magnetic field

Now we consider a single solenoid inside an homogeneous magnetic field of amplitude H_{ext}, oscillating at frequency f and parallel to the solenoid's axis. The solenoid is connected in series to a variable capacity C and an ohmic resistance R, forming an RCL circuit. The oscillating current $I_{ind} = I_{ind}(f,H,C)$ induced in the solenoid creates a scattered electromagnetic field with components

$$H_r^{scatt-PW}(f,H,\theta,r,C) = H_r(f, I_{ind}(f,H,C), \theta, r),$$
$$H_\theta^{scatt-PW}(f,H,\theta,r,C) = H_\theta(f, I_{ind}(f,H,C), \theta, r)$$
$$E_\phi^{scatt-PW}(f,H,\theta,r,C) = E_\phi(f, I_{ind}(f,H,C), \theta, r).$$

The extension PW stands for plane-wave.

In Figure 5 we show the Poynting-field lines calculated from these scattered fields, with L, C and the resonant frequency f_{res} of the equivalent RCL circuit given in section 1. The frequencies shown are at $f = 0.90\, f_{res}$, $f = f_{res}$ and $f = 1.10\, f_{res}$. Notice the clear qualitative change of the Poynting flux lines at fres with respect to the cases with $f = f_{res}$. This is due to the fact that, at resonance, it is the real part of the oscillating induced current that dominates (similarly to the case when the fields stem from an imposed real current in the solenoid, as in section 3), whereas the imaginary part of Iind dominates away from fres . The fact that the external field is homogeneous and oriented along OZ implies that, at all frequencies, the scattered magnetic and Poynting flux diagrams in the XZ plane exhibit a $X \to -X$ symmetry and there is no net power flux along X.

The full power fluxes $\vec{P}$ are the sum of the scattered Poynting fields $\vec{P}_{scatt}$ shown above and the power fluxes $\vec{P}_{ext}$ associated to the externally imposed magnetic field $\vec{H}_{ext}$:

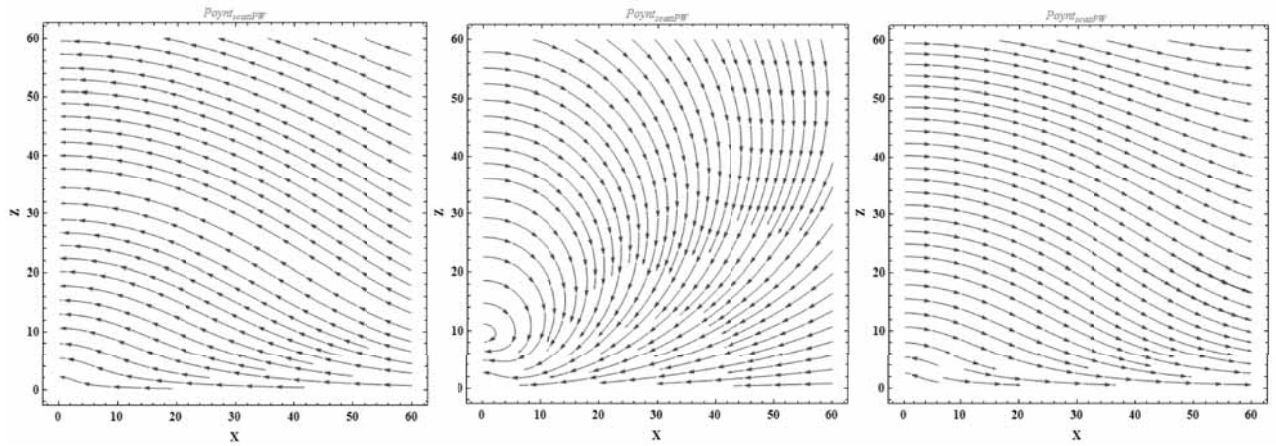

Figure 5: Scattered Poynting-vector fluxes at $f < f_{res}$ (upper left), $f = f_{res}$ (upper right) and $f > f_{res}$ (bottom).

$$\vec{P} = \vec{P_{ext}} + \vec{P}_{scatt}$$

Clearly, an harmonic external pure magnetic field $\vec{H}$ which is spatially homogeneous will carry no power flux, not only for reasons of symmetry (in which direction would the flux be oriented ?) but also because an electric field is needed to create a Poynting vector. Last, but not least, such a pure magnetic field does not exist, according to Faraday's law

$$rot\,\vec{E}_{ext}(\vec{r},t) = -\frac{\partial \vec{B}_{ext}(\vec{r},t)}{\partial t} \tag{7}$$

where $\vec{E}_{ext}$ is the induced external electric field and $\vec{B}_{ext} = \mu_0 \vec{H}$ is the external *magnetic induction* field.

3.2 Near plane-wave external magnetic field

We assume that $\vec{B}_{ext}$ varies harmonically in time that is, $\vec{B}_{ext}(\vec{r},t) = \vec{B}_{ext}(\vec{r})\, e^{\imath\,\omega\, t}$. Then, by linearity, $\vec{E}_{ext}$ and $\vec{B}_{ext}$ will have the same dependency on t and equation (7) reduces to

$$rot\,\vec{E}_{ext}(\vec{r}) = -\imath\,\omega\,\vec{B}_{ext}(\vec{r}) \tag{8}$$

We make the further assumptions that $\vec{B}_{ext}$ is everywhere oriented along OZ and that its eventual variations are along OXs that is, $\vec{B}_{ext}(\vec{r}) = \{0,0,B_0(x)\}$. Then, if we restrict ourselves to the OXZ-plane, where $\vec{E}_{ext}$ has only a y-component ($E_x = E_z = 0$), then equation 8 becomes

$$\frac{d\vec{E}_{ext}(x)}{dx} = -\imath\,\omega\,\vec{B}_0(x) \tag{9}$$

Were $B_0(x)$, and thus $\vec{B}_{ext}$, constant, the resulting electric field would have $E_y(x) = -\imath\,\omega\,B_0\,x + E_y^{(o)}$. Therefore it would become arbitrarily large at sufficiently large x, which is physically unacceptable. To avoid this, we introduce a x-dependency in $\vec{B}_{ext}$ in such a way that $\vec{B}_{ext}$ is almost uniform in the region surrounding the solenoid.

Furthermore, to have a globally net power flux, this magnetic field will be a planewave magnetic for which we define a propagation direction, sense and wavenumber $k = \frac{2\pi}{\lambda}$, by means of a wave-vector $k = k\,\vec{u}$, with $\vec{u}$ the unitary vector giving the magnetic wave direction and sense. Consider thus the following external magnetic-induction field $\vec{B}_{ext}(\vec{r}) = \{0,0,B_0(x)\}$ with

$$B_0(x) = b_0\, e^{-\frac{(x-x_0)^2}{2\,\sigma^2} - \imath\,k\,x} \tag{10}$$

and the induced field is $\vec{E}_{ext}(\vec{r}) = \{0,E_y(x),0\}$, with

$$E_y(x) = -b_0 \sqrt{\frac{\pi}{2}}\, e^{-\frac{1}{2}\,k^2\,\sigma^2}\,\sigma\,\omega\, Erfi\left(\frac{\imath\,x - k\,\sigma^2}{\sigma\sqrt{2}}\right) \tag{11}$$

and $Erfi$ is the imaginary error function, $Erfi(z) = -\imath\, erf(\imath\, z)$.

For an external magnetic induction of amplitude $b_0 = 1\,[T]$, with a spatial spread of $\sigma = 70\,[m]$ oscillating at the resonating frequency $f_{res} = 998'649\,[Hz]$, the Poynting vector $\vec{P}_{ext} = Re[E_y(x,\sigma,k,b_0)] \cdot Re[B_0(x,\sigma,k,b_0)/\mu_0]$ is aligned in the positive X-direction and varies slowly in x with a scalar value close to $P_x^{(o)} = 1.35 \times 10^{-4}\,[W/m2]$.

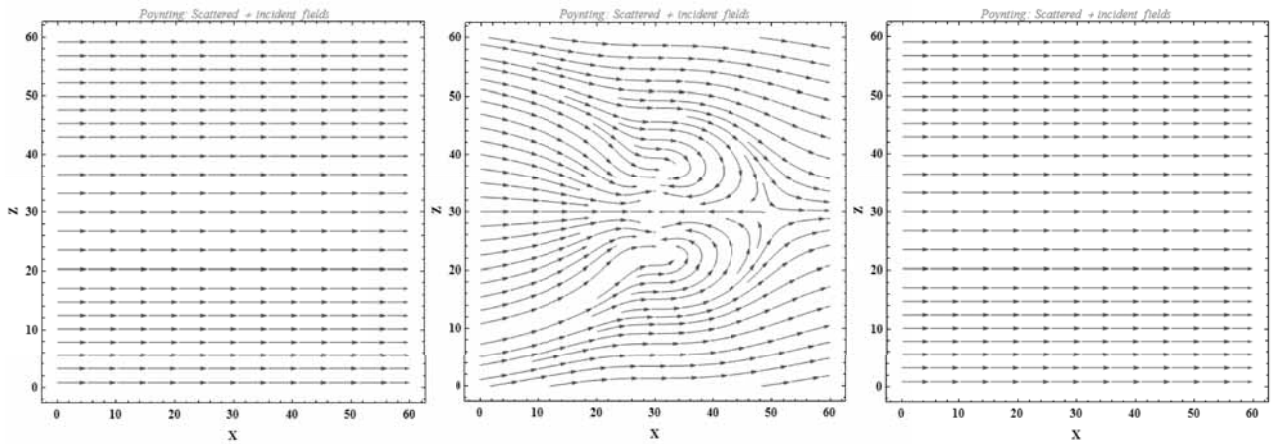

Figure 6: Power flux lines in the XZ-plane at frequencies $0.90\,f_{res}$ (left), f_{res} (center) and $1.10\,f_{res}$ (right). The field arrows are not drawn to scale, they only show the local field directions. Notice that the solenoid's centre is now at $x_0 = z_0 = 30\,[m]$.

The superposition of this external Poynting field and the scattered one is shown in Figure 6 at frequencies $0.90\,f_{res}$, f_{res} and $1.10\,f_{res}$. The concentration of flux lines is particularly strong at resonance. Away from the resonance, this effect is either absent (low-f) or less pronounced (high-f).

4 Poynting Concentration, Resonance and Total Absorption

The clear convergence of the Poynting flux lines around the solenoid at resonance with an external magnetic field is related to the sharp increase of power transfer from the external field to the RCL circuit of the solenoid at resonance. A similar phenomenon occurs in optics when a monochromatic light beam incident upon a completely absorbing full disk produces a bright and tiny spot (Poisson-Arago spot) behind the disk, at the centre of the circular shadow region [4]. Another well-known effect is the sudden opacity developed by a cloud of micron-sized metallic particles when the frequency of the incident light coincides with the frequency of resonances due to plasmon oscillations on the particles' surfaces.

We also simulated the concentration of power flux around a small absorbing sphere placed in an electromagnetic field at resonance with the sphere's plasmon oscillations, as shown in Figure 7. The numerical calculation was done with finite elements using Comsol.

At the resonant frequencies, the target (solenoid, dark disk, particle) behaves like a larger object from the point of view of the total power flux geometric distribution [2], [8]. The wave nature of the surrounding fields is essential for explaining these power concentration effects since the wave-fronts are deformed to satisfy the constraints imposed by the condition of total absorption at the target. Put differently, the target is actually the source of a scattered wave field which interferes with the external field and produces convergent Poynting around the target.

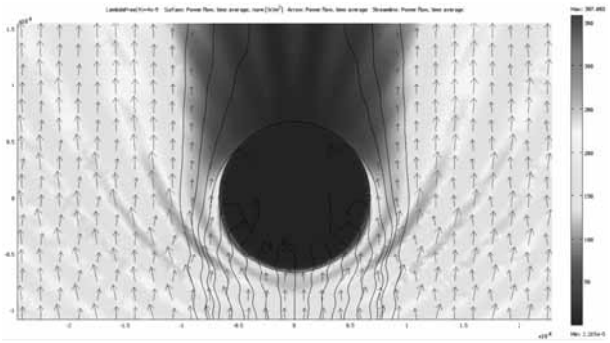

Figure 7: Strong absorption of an EM wave of wavelength $\lambda = 4\,[nm]$ by a spherical particle with a diameter of $15\,[nm]$: Black full lines represent Poynting flux, with norm indicated by the background colours. Arrows represent the Poynting vectors.

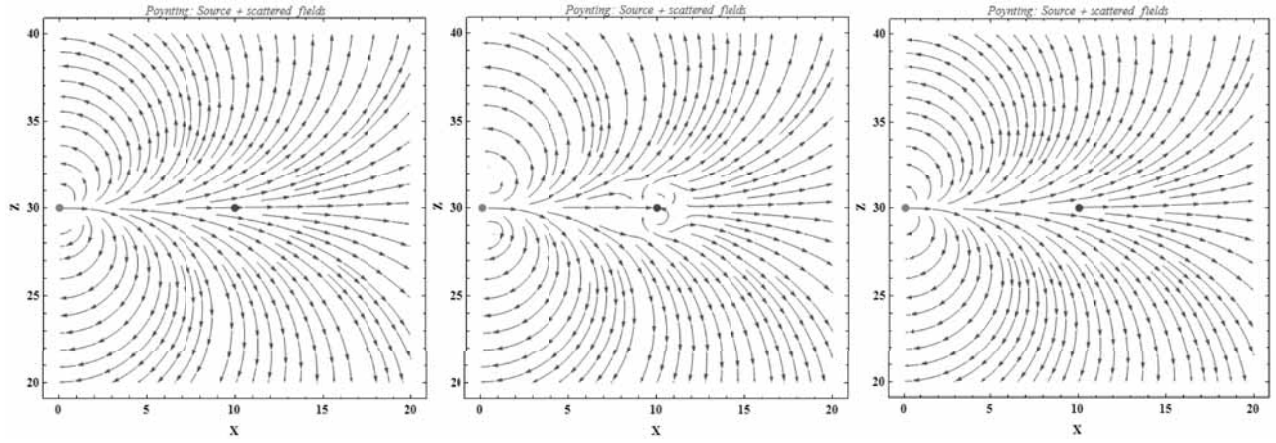

Figure 8: Total power flux lines for the sum of the source (left coil in each diagram) and target (right coil) Poynting vectors fields. The frequencies are $0.90\, f_{res}$ (left), f_{res} (centre) and $1.10\, f_{res}$ (right). We assume that the left coil (source) contains only the external current (i. e., no self- or mutually-induced currents). The power flow is then one-way and the resonance frequency of the pair of coils stays equal to fres, otherwise there would be resonance-splitting. The left (right) fat dot represents the source (target) coil.

5 Mutually Coupled Coils

If the resonating coil of section 3.2 is now placed inside a magnetic field created by a single coil with current oscillating at frequency f_{res} (as in section 2.1), it is reasonable to expect that the same type of concentration of power flux lines will occur around the resonating coil, as seen in section 3.2. This is confirmed by the present model as can be observed from the shape of the Poynting flux lines at $f = f_{res}$, in Figure 8, which form a sort of tube between the source at left and the target coil at right (middle of the central diagram).

In this calculation we used an unreasonably large distance ($10\,[m]$) between the source and the target coils to emphasize the presence of this power transfer mechanism even when that distance is large compared to the coils' dimensions. It should be stressed that the source-target distance is nevertheless smaller than the typical size of the *near-field* zone, $\frac{\lambda}{2\,\pi} \approx 50\,[m]$. In this zone, the fields are normally *evanescent* that is, their amplitudes decrease very fast with the distance from the source and they do not radiate.

If there is a region where the flux lines are tubular however, as happens at $f = f_{res}$, the power flux density decreases less rapidly in that region than what is expected to happen with evanescent, non-radiative fields. It is as if a limited region of radiative far-field was brought inside the near-field zone. These model results are in qualitative agreement with the literature on wireless power transfer already cited.

The role of the high quality factor Q of the oscillating circuits involved should now be clear, given the extreme sensitivity of the power-flux concentration effect with respect to the frequency f : Frequency shifts of 10% around the resonance f_{res} - and actually much less than that - completely wipe-out all traces of the Poynting field convergence effect. Resonant circuits with small values of Q won't have enough frequency stability to allow for the observation of this effect. The quality factor of our model resonating target coil is very high: $Q \approx \omega_{res}\, \frac{L}{R} \approx 3'620$.

The same concentration of flux lines occurs when the source and target coils are not placed in the same plane, as is shown in Figure 9, where the upper row diagrams correspond to axial coils and the lower row to a more general geometry, with the coils' axis remaining however parallel.

6 Applications

The idea of transferring electromagnetic power over long distances is an old one, going back to Tesla in the late nineteenth century. His ideas actually inspired the MIT team [7], [6]. Since the publication of these later works, a large number of publications appeared in parallel with various proposals for industrial applications. The literature on this subject is by now quite extensive. Some reviews can be found at [10] and on the Web [11], [5] , [9] (with many references and patent listing).

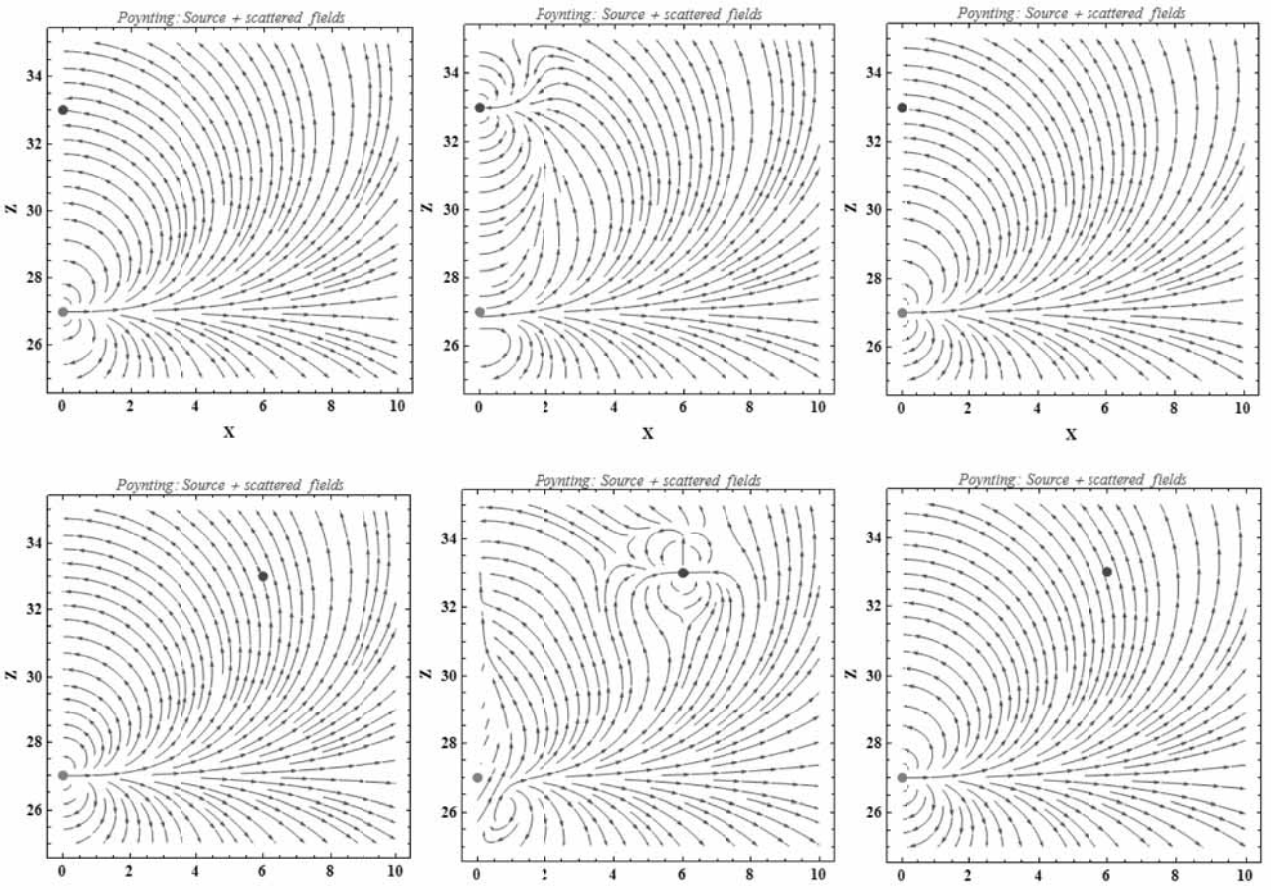

Figure 9: Generation of power-flux tubes under more general source / target geometries.

The same physical mechanism that underlies power transfer and which was modelled here could also be used in principle, for the transfer of information. In fact the RFID devices use the same principle of mutual induction between magnetically coupled oscillating circuits. There is however an important difference between RFID's functioning and the present schemes: RFIDs contain relatively low Q (quality-factor) oscillators, which makes them quite insensitive to small frequency changes between source and tar- get. For the phenomena discussed here, on the contrary, strong resonance (akin to total absorption) is critical to producing clear power flux concentration.

7 Conclusions

1. A clear transition was modelled and occurs in the spatial pattern of electromagnetic power flux when a solenoid is embedded in an harmonic magnetic field oscillation exactly at the frequency of resonance of the solenoid circuit. At this frequency, the power flux lines crossing a region surrounding the solenoid tend to converge very strongly past the solenoid, in sharp contrast to what is observed away from resonance, where the flow patterns are only mildly affected by the solenoid oscillating circuit.
2. This phenomenon was studied with the help of an analytical model using the program *Mathematica*. In this model, the interactions between the different subsystems (coupling between fields and currents) was interpreted under the form of hierarchies of functions whose arguments were other functions.
3. Power concentration related to strong absorption was related to other well known phenomena found in different areas of Physics. A numerical simulation by finite elements, made using the program *Comsol*, numerically confirmed the power concentration effect. Finally, the basis of the effects was argued to be the wave nature of the fields involved.

Acknowledgement

The author thanks Patrick Favre and Dominique Bovey for useful discussions.

References

[1] Balanis, CA. *Antenna Theory - Analysis and Design*. Edition 1. New York: Harper and Row; 1982. 816 p.

[2] Bohren CF. How can a particle absorb more than the light incident on it?. *Am J Phys*. 1983; 51(4):323–327. doi:10.1119/1.13262.

[3] Feng Y, Braaten B, Nelson R. Analytical expressions for small loop antennas - with application to emc and rfid systems. In IEEE. EMC 2006 Proceedings Volume 1. *2006 IEEE International Symposium on Electromagnetic Compatibility*; 2016 Aug; Portland, Oregon USA. 445 Hoes Lane, Piscataway, NJ 08855-1331 USA : IEEE. 63-68. doi:10.1109/ISEMC.2006.1706264.

[4] Gondran M, Gondran A. Energy flow lines and the spot of Poisson-Arago. *Am J Phys*. 2010; 78(6):598–602. doi:10.1119/1.3291215

[5] *Intel's Wireless Power Technology Demonstrated*. http://thefutureofthings.com/news/5763/intel-s-wireless-power-technology-demonstrated.html 2009.

[6] Karalis A, Joannopoulos JD, Soljacic M. Efficient wireless non-radiative mid-range energy transfer. *Annals of Physics*. 2008; 323:34–48. doi:10.1016/j.aop.2007.04.017

[7] Kurs A, Karalis A, Moffatt R, Joannopoulos JD, Fisher P, Soljacic M. Wireless power transfer via strongly coupled magnetic resonances. *Science*. 2007; 317:83. doi:10.1126/science.1143254

[8] Paul H, Fischer R. Comment on "how can a particle absorb more than the light incident on it?". *Am J Phys*. 1983; 51(4):327. doi:10.1119/1.13471

[9] PowerPedia. Wireless transmission of electricity. http://peswiki.com/index.php/Powerpedia:Wireless_transmission_of_electricity.

[10] van Bussel R, Franken j, Golchin S, Leijenaar R. Wireless Power Supply. MDP1, Final report (V. 2) 14-12-2007, 2007.

[11] Wireless Electricity. http://emergingtechnology.wordpress.com/2007/10/02/wireless-electricity. 2007.